Structural Evolution Governs Reversible Heat Generation in Electrical Double Layers

Liang Zeng, Ming Chen, Zhenxiang Wang, Rui Qiao, and Guang Feng

Structural evolution governs reversible heat generation in electrical double layers

Liang Zeng[1], Ming Chen[1], Zhenxiang Wang[1], Rui Qiao[2], and Guang Feng[1,*]

[1]*State Key Laboratory of Coal Combustion, School of Energy and Power Engineering, Huazhong University of Science and Technology, Wuhan 430074, China*
[2]*Department of Mechanical Engineering, Virginia Tech, Blacksburg, VA 24061, USA*
[*]Correspondence: gfeng@hust.edu.cn

Electrical double layer (EDL) formation determines the reversible heat generation of supercapacitors. While classical theories suggest an exothermic nature, experiments revealed that it can be endothermic, depending on the polarization and electrolyte. Here, we performed constant-potential molecular dynamics simulations and developed a lattice gas model to explore the reversible heat of EDL formation in aqueous and ionic liquid (IL) electrolytes. Our work reveals that EDL formation in aqueous electrolytes exhibits endothermicity under negative polarization; it shows new complexity of endothermicity followed by exothermicity in ILs, regardless of electrode polarity. These thermal behaviors are determined by the structural evolution during EDL formation, dominated by adsorbed solvent molecules rather than ions in aqueous electrolytes but governed by "de-mixing" and "vacancy occupation" phenomena in ILs. This work provides new insights into the reversible heat of supercapacitors and presents a theoretical approach to investigating thermal behaviors involving the dynamics of EDLs.

Introduction. – Supercapacitors, storing charge in electrical double layers (EDLs) at electrode-electrolyte interfaces, have emerged as a key energy storage technique due to their high power density and superior cyclability[1-3]. Their progress, however, inadvertently brings new challenges. Heat is inevitably generated when charging and discharging supercapacitors, more so as power and energy densities improve[1,4-7]. Each improvement in those regards tends to exacerbate thermal issues in supercapacitors, which can impair their performance, cyclability, and safety[1,5,7].

Heat generation in supercapacitors features irreversible and reversible parts[4,5,8-11]. The irreversible heat is exothermic and has been well-understood to originate from Joule heat[4,5,9,12]; the reversible heat, however, exhibits much richer behaviors. Early experiments lumped the heat generation of positively and negatively polarized electrodes together. When aqueous electrolytes were used, the net reversible heat is exothermic during charging (i.e., EDL formation) and the opposite during discharging[8,10]. Similar exothermicity was reported for organic[5] and ionic liquid (IL)[11] electrolytes. Recent measurements distinguished heat flow in negative and positive electrodes, revealing that EDL formation under positive polarization is exothermic, independent of electrolyte type[9,11,13]. However, under negative polarization, EDL formation is fully endothermic in aqueous salt electrolytes[13], but can be partially endothermic in aqueous acid and IL electrolytes, depending on electrical potential[9,11]. Based on kinetics[4,12,14] and thermodynamics[4,5,15-17] considerations, theories predict exothermicity for EDL formation and attribute it to the entropy decrease resulting from the increased ordering of ions in EDLs under polarization[4,5]. Meanwhile, exothermic heat was predicted to decrease with increasing ion concentration of bulk electrolyte by theories combining Poisson-Nernst-Planck and heat conduction equations[14], while calorimetric experiments reported concentration-insensitive heat generation[10]. The endothermic heat under negative polarization was recently predicted by classical density functional theory[18], which remains to be further tested. Therefore, current theories cannot yet fully elucidate different behaviors of reversible heat, from its endothermicity to its dependence on ion concentration, electrolyte type, and electrode potential.

In this Letter, we employed constant-potential molecular dynamics (MD) simulations[2,19,20], which provide atomistic-level descriptions for EDL formation and explicit thermal signals[6,19], to investigate reversible thermal behaviors of EDLs in aqueous and IL electrolytes. Unlike the widely reported exothermic behaviors[4,5,10,12,14,15], our work reveals an endothermic and ion concentration-insensitive process of EDL formation in aqueous electrolytes under negative polarization. It uncovers new complex behaviors of endothermicity followed by exothermicity during EDL formation in ILs depending on the electrical potential, independent of the electrode polarity. To rationalize this reversible heat, we developed a modified lattice gas model incorporating translational and orientational entropy to bridge the macroscopic thermal phenomena and the microstructural evolution of EDLs.

Thermal behaviors.– Supercapacitors are constructed as MD systems with aqueous NaCl solutions or IL (1-ethyl-3-methylimidazolium tetrafluoroborate, [EMIM][BF$_4$]) enclosed between two planar electrodes (inserts in Fig. 1). The systems, starting at a voltage of 0 V, were charged under isothermal conditions with a temperature of T_0 by linearly ramping up the voltage slowly to minimize irreversible heat. Simulation details are given in Sections 1-2 of Supplemental Material (SM)[21].

For systems with aqueous electrolytes of different ion concentrations, MD simulations show that the net heat flowing into the system, Q_{rev}, is negative and monotonically decreases with time t [corresponding to the applied voltage, U, Fig. 1(a)], indicating that charging is exothermic, consistent with classical theories[4,12] and previous experiments[8,10]. Q_{rev} is insensitive to ion concentration, in line with experimental measurements with the same aqueous electrolyte[10], implying that ions may play a minor role in reversible heat. Very different from aqueous systems [Fig. 1(b) *vs.* 1(a)], Q_{rev} obtained from MD simulations of IL systems mostly increases with polarization at voltages below ~2 V, suggesting an endothermic process in EDL formation, which has never been described by any theoretical work. At voltages over ~2 V, charging becomes exothermic. The same conclusions can be drawn from aqueous and IL systems operated under adiabatic conditions, and the simulation reliability has been validated (Section 3 of SM[21]).
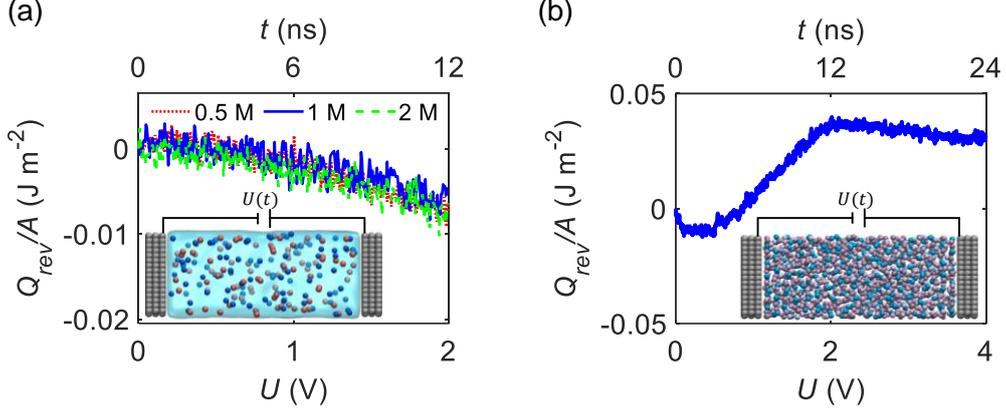
FIG. 1. Area-normalized reversible heat (Q_{rev}/A) flowing into supercapacitors during isothermal charging. Inserts show the molecular rendering of supercapacitors with aqueous NaCl solution (a) and IL [EMIM][BF4] (b). A is the electrode surface area. In (a), blue (red) spheres are cations (anions), and the translucent blue is water. In (b), pink (light blue) spheres are cations (anions). Electrodes are gray.

Origins of endothermicity in aqueous electrolytes.– Reversible heat is determined by the entropy change of the system during charging/discharging[4,10]. The exothermic reversible heat indicates that, relative to its initial state at $U = 0$ V, the cumulative system entropy change (calculated as $\Delta S_{MD} = Q_{rev}/T_0$) decreases monotonically with U [Fig. 2(a)]. To delineate the relationship between ΔS_{MD} and U obtained in MD simulations, we developed a lattice gas model to quantify the system entropy. Our lattice gas model adds an orientational entropy[22] (S_{LG}^{or}) to the translational entropy (S_{LG}^{tr}) considered in classical lattice gas models[3,23-26]:

$$S_{LG} = S_{LG}^{tr} + S_{LG}^{or}. \tag{1}$$

Herein, S_{LG}^{tr} is determined by density distributions and given by

$$S_{LG}^{tr} = \int -k_b \left(\rho_+ \ln \frac{\rho_+}{\rho_{max}} + \rho_- \ln \frac{\rho_-}{\rho_{max}} + \rho_{sol} \ln \frac{\rho_{sol}}{\rho_{max}} + \rho_{vac} \ln \frac{\rho_{vac}}{\rho_{max}} \right) dV, \tag{2}$$

where k_b is the Boltzmann constant; ρ_+, ρ_-, and ρ_{sol} are the local number densities of cations, anions, and solvent molecules, respectively, ρ_{max} the maximal number density (vacancy density is $\rho_{vac} = \rho_{max} - \rho_+ - \rho_- - \rho_{sol}$), V the volume. S_{LG}^{or} comes from molecular orientation distributions, as

$$S_{LG}^{or} = \sum_l^{+,-,sol} \int -k_b \left[\rho_l \int_0^\pi \cdots \int_0^\pi f_l(\theta_1, \dots, \theta_n) \ln f_l(\theta_1, \dots, \theta_n) d\theta_1 \dots d\theta_n \right] dV, \tag{3}$$

where $f_l(\theta_1, \dots, \theta_n)$ is the probability density function describing the orientational distribution of component l (cation, anion, or solvent), and $\theta_1, \dots, \theta_n$ are the angles that

4

characterize the molecule's orientational state. Details of the modified lattice gas model are given in Section 4 of SM[21].
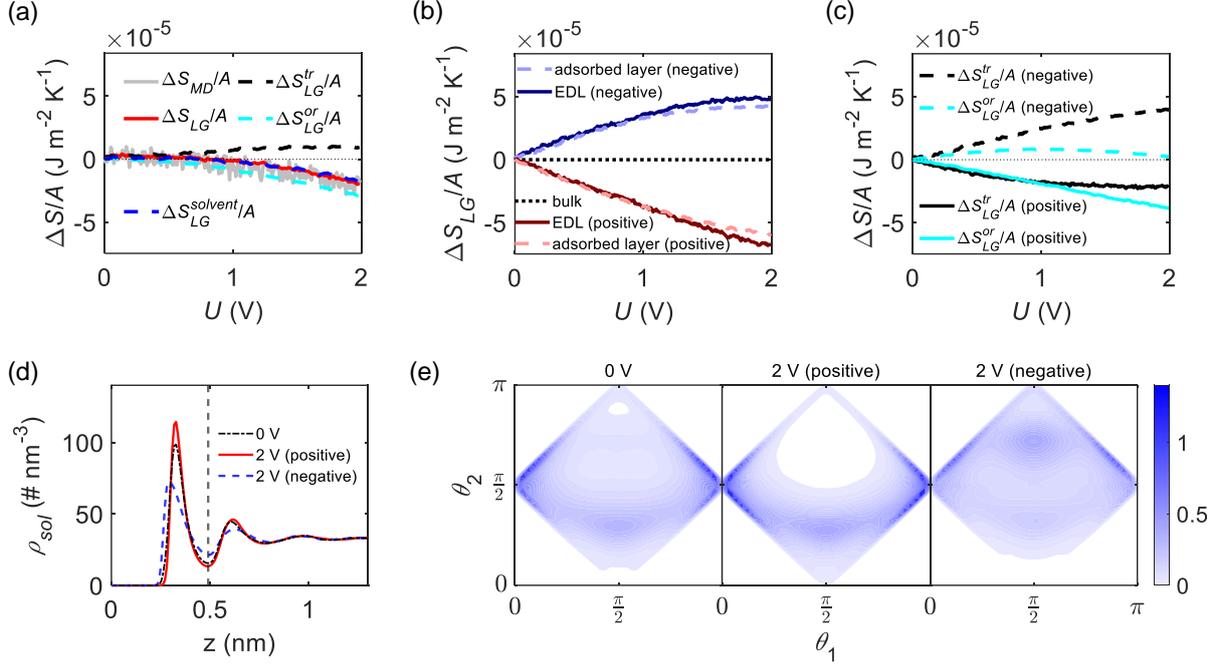

FIG. 2. Origins of reversible heat of EDLs in aqueous electrolytes. (a) Cumulative system entropy change per electrode area during isothermal charging obtained from MD simulations ($\Delta S_{MD}/A$) and the modified lattice gas model ($\Delta S_{LG}/A$) consisting of $\Delta S_{LG}^{tr}/A$ and $\Delta S_{LG}^{or}/A$. $\Delta S_{LG}^{solvent}$ is the system entropy change associated with solvent molecules alone. (b) $\Delta S_{LG}/A$ of regions of EDLs and adsorbed solvent layer at negative and positive electrodes, and that of bulk electrolyte. (c) $\Delta S_{LG}^{tr}/A$ and $\Delta S_{LG}^{or}/A$ of the adsorbed solvent layer. (d) Solvent number density as a function of distance from the electrode. (e) Probability density distribution for the orientation of adsorbed solvent molecules.

Using density and orientation distributions from MD simulations, the entire system's entropy change and reversible heat during EDL formation can be captured by the modified lattice gas model but not by the classical model with only translational entropy [Fig. 2(a)], implying that translational and orientational entropies both play significant roles. After verified by MD simulations for the total reversible heat, the modified lattice gas model is employed to understand the origin of the reversible heat in EDLs near positive and negative electrodes separately.

Previous theories for reversible heat attributed the system entropy reduction with an applied voltage to increased ion concentrations at electrode-electrolyte interfaces[4,5]. Here, we evaluate the entropy change associated with ions and solvent molecules. The system entropy

change due to solvent, $\Delta S_{LG}^{solvent}$, was calculated by Eqs. S(12-13) and found to be almost identical to that based on ions and solvent molecules together [Fig. 2(a)]. This suggests that for our systems with *concentrated* aqueous electrolytes and *high* voltage, solvent molecules rather than ions dominate system entropy change during EDL formation, which could be ascribed to the more substantial variation of solvent density than ion density (Fig. S8).

The reversible heat of EDLs formed at either negative or positive electrodes is exothermic in classical theory[4,5,10,12], while a very recent experiment found it is endothermic under negative polarization[13]. To examine this contradiction, we utilize the modified lattice gas model to partition the system into three parts: regions of EDLs at negative/positive electrodes and bulk electrolytes (Fig. S9). The entropy changes in different regions show that the EDL formation is exothermic under positive polarization and endothermic under negative polarization [Fig. 2(b)], in agreement with the experiment[13]. Further, the entropy change of the whole EDL is very close to that of the solvent layer adsorbed on the electrode, implying the dominance of the adsorbed solvent layer as it exhibits the drastic structural changes during EDL formation [Fig. 2(d)].

Using Eq. (1), entropy changes of the adsorbed solvent layer were further separated into translational and orientational parts [Fig. 2(c)], which could be understood by their structural evolution in terms of density and orientation distributions, respectively. Based on Eq. (2), given analytical density profiles with a similar amount of adsorbed solvent molecules (Section 6 of SM[21]), translational entropy decreases as solvent molecules become more tightly arranged (higher density peak) and increases with less packed solvent (lower density peak). Therefore, as shown in Fig. 2(d), the density peak of the adsorbed layer increases (decreases) with positive (negative) polarization, leading to a decrease (increase) of the translational entropy [Fig. 2(c)].

Following Eq. (3), the evolution of the orientational entropy of the adsorbed solvents [Fig. 2(c)] can be understood by studying their orientational distributions. The latter is quantified as a function of the angle between the electrode's normal vector and the water plane's normal vector (θ_1) and the angle between the electrode's normal vector and the water dipole (θ_2). Fig. 2(e) shows that, at 0 V, the adsorbed water molecules prefer to align parallel to the electrode

6

surface (θ_1 near 0 and π with θ_2 at $\sim\pi/2$), although their orientational states span almost the entire possible range [see the square region in the map, left panel of Fig. 2(e)]. When the polarization increases from zero, more water molecules align parallel to the electrode surface, and the accessible orientational states are significantly reduced [almost no water in the region of $\pi/4 < \theta_1 < 3\pi/4$ and $\pi/2 < \theta_2 < \pi$, left vs. middle panels in Fig. 2(e)]. These changes indicate that the adsorbed solvent layer becomes more ordered, resulting in a decrease in its orientational entropy [Fig. 2(c)]. When the polarization decreases from zero, although some water molecules switch from the parallel to a vertical configuration, the peak and overall accessible state space of orientational distributions do not vary much [left vs. right panels in Fig. 2(e)], which leads to the weak change in the orientational entropy [Fig. 2(c)].

Therefore, the exothermicity of EDL formation under positive polarization is attributed to the simultaneous reduction of translational and orientational entropies associated with the rearrangement of adsorbed solvent molecules. Under negative polarization, the solvent rearrangement leads to an increase in translational entropy and a slight change in orientational entropy, resulting in endothermicity [Figs. 2(b), 2(c)].

The structure of the solvent in the EDL region was further found to be almost independent of the ion concentration, although the ion density in EDL varies dramatically with bulk ion concentration (Fig. S12); hence, the dominance of adsorbed solvent helps clarify why reversible heat are insensitive to ion concentration, as observed in previous experiments[10] and our simulations [Fig. 1(a)].

Mechanisms of endothermicity in ILs.– We now focus on reversible heats of the solvent-free IL system, which have not been theoretically studied. The system entropy change, computed from the reversible heat measured in MD simulations[Fig. 1(b)], was found to vary non-monotonically with U [Fig. 3(a)]. Using the EDL structures from MD simulations, the system entropy change was further calculated using the modified lattice gas model. The reasonable agreement between ΔS_{MD} and ΔS_{LG} [Fig. 3(a)] demonstrates that the modified lattice gas model also performs well for IL systems. Particularly, for the contribution of translational and orientational parts, in sharp contrast to aqueous electrolyte systems, the variation in

7

translational entropy dominates the system entropy change [Fig. 3(a)], likely due to substantial variations in ion densities [Figs. 3(b), S13].
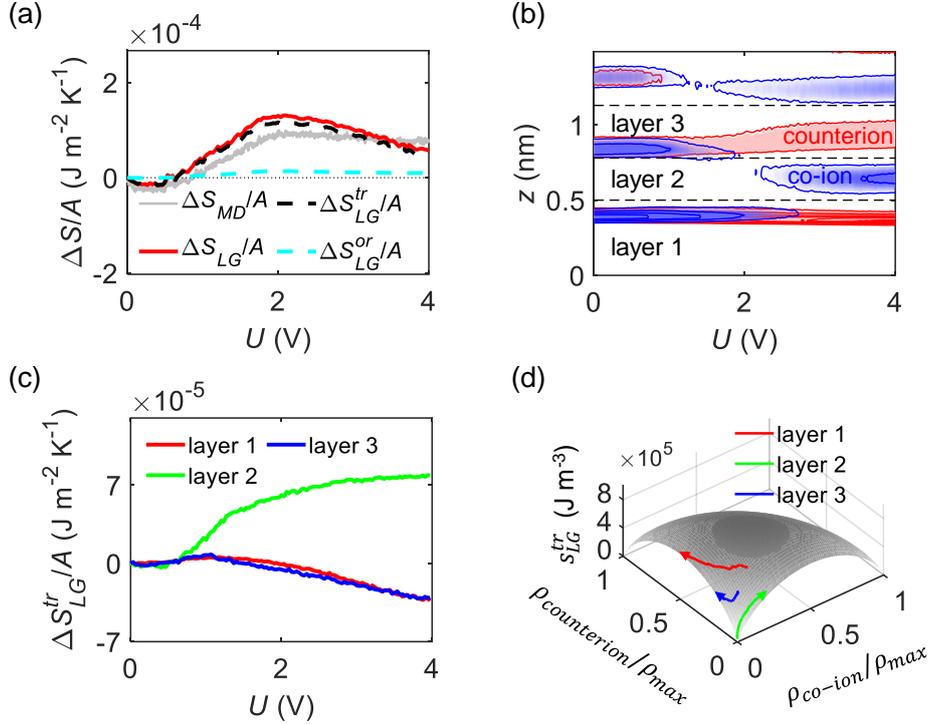

FIG. 3. Origins of reversible heat of EDLs in ionic liquids. (a) Cumulative system entropy change per electrode area during the charging process from MD simulations ($\Delta S_{MD}/A$), and from the modified lattice gas model ($\Delta S_{LG}/A$) consisting of $\Delta S_{LG}^{tr}/A$ and $\Delta S_{LG}^{or}/A$. (b) Number densities of co-ions (blue area) and counterions (red area) with voltage and distance from the negative electrode. The contour interval is $1.5\rho_{bulk}$ (ρ_{bulk}: ion density of bulk electrolyte); the first contour starts at $1.5\rho_{bulk}$, and the last contour represents densities higher than $9\rho_{bulk}$. Three ion layers near the electrode are divided by ion density valleys (dashed lines). (c) $\Delta S_{LG}^{tr}/A$ of ion layers near the negative electrode. (d) Dependence of translational entropy density, s_{LG}^{tr}, on ion densities in the lattice gas model [expressed by the integrand of Eq. (2)]. The solid color lines with arrowhead represent the evolution of ionic peak number densities.

To explore the effect of electrode polarity, we analyze the contribution of translational entropy change of EDLs for negative and positive electrodes using the modified lattice gas model (Figs. S14-15). The entropy changes demonstrate that EDL formations are both endothermic at first, then become exothermic, in contrast to aqueous systems. The same trend of entropies under negative and positive polarizations could be ascribed to the similar evolution of EDL structures [Fig. 3(b) *vs.* Fig. S13].

Differing from aqueous EDLs with entropy change dominated by the adsorbed solvent layer [Fig. 2(b)], the entropy change of IL-based EDLs is mainly governed by the first three ion layers near the electrode [Fig. 3(b) and Figs. S13-15]. Figures 3(c-d) show that the translational entropy changes of these ion layers under negative polarization are determined by density variations of counterions and co-ions, which differs fundamentally from the dominance by solvents in aqueous EDLs. Specifically, translational entropies of these ion layers vary slightly under small voltage [$U <\sim 0.6$ V, Fig. 3(c)] due to the marginal change of ion densities [Fig. 3(b), Fig. S16(a)]. When $U >\sim 0.6$ V, the entropy of ion layer 1 decreases with U [Fig. 3(c)], which can be attributed to the "de-mixing" of counterions and co-ions[27,28]: counterions are significantly added, and co-ions are simultaneously removed and eventually depleted [Figs. 3(b), 3(d) and Fig. S16(a)]. This de-mixing drives layer 1 from a two-component to a single-component state, consequently reducing the entropy[28] [Fig. 3(d)] . The mechanism of ion de-mixing also explains the entropy decrease in ion layer 3. For ion layer 2, the entropy increases with U [Fig. 3(c)], which originates from the "vacancy occupation":[25] as shown in Fig. 3(b) and Fig. S16(a), there is almost no ion between ion layer 1 and 3 under small voltage, and co-ions gradually occupy this vacancy with increasing voltage, increasing the entropy greatly [Fig. 3(d)].

Overall, driven by the competition between the "de-mixing" and "vacancy occupation", EDL formation is endothermic and then exothermic with increasing voltage (Fig. S15): when $U <\sim 1.5$ V, the entropy increase due to "vacancy occupation" dominates over the entropy decrease due to "de-mixing"; the opposite occurs for $U >\sim 1.5$ V [Fig. 3(c) and Fig. S17(a)].

The EDL structural evolution near the positive electrode is similar to that near the negative electrode. Hence the entropy changes of ion layers follow the same "de-mixing" and "vacancy occupation" mechanisms. Therefore, the entropy change under positive polarization resembles that under negative polarization (Figs. S13-18).

Discussion.– Reversible heat of supercapacitors with typical aqueous and IL electrolytes are investigated by MD simulations and scrutinized by a modified lattice gas model incorporating translational and orientational entropies. We show that EDL formations in supercapacitors with

aqueous and IL electrolytes can be endothermic, contrary to the prediction by classical theories[4,5,10,12].

Although an overall exothermicity is observed for supercapacitors featuring aqueous electrolytes, EDL formation under negative polarization is endothermic. These rich thermal behaviors are dominated by solvent molecules rather than ions, which classic EDL theories cannot describe. This is probably because the electrolytes studied here are not dilute[29], and the applied voltage far exceeds the thermal voltage[30]. The structural evolution of the adsorbed solvent layer, in terms of density and orientation, governs thermal behaviors: adsorbed solvent molecules are packed more disorderly under negative polarization, resulting in endothermicity, and more orderly under positive polarization, causing exothermicity.

The EDL formation in IL electrolytes is endothermic and then exothermic, varying with polarization; the net reversible heat is endothermic at voltage up to 4 V. These complex thermal behaviors are understood by the ion addition and removal during EDL formation: the "de-mixing" of counterions and co-ions promotes exothermicity, and ions' "vacancy occupation" drives endothermicity. These results may be tested by calorimetric experiments combined with surface force apparatus, scanning probe microscopy, or surface-sensitive nonlinear optical techniques[7,31].

This work advances the understanding of supercapacitors' rich thermal behaviors and helps extract microscopic information about EDLs from thermal signals[4,10]. It could also help understand the thermal behaviors of other EDL-related fields, such as batteries[32,33], capacitive deionization[16], low-grade heat harvesting[16,17], and nervous conduction[15]. This work focuses on planar electrode systems, and future investigations could shift towards realistic nanoporous electrode systems taking nanoconfinement effects on thermal behaviors[1-3].

[1]   P. Simon and Y. Gogotsi, Nat. Mater. **19**, 1151 (2020).

[2]   G. Jeanmairet, B. Rotenberg, and M. Salanne, Chem. Rev. **122**, 10860 (2022).

[3]   J. Wu, Chem. Rev. **122**, 10821 (2022).

[4]   M. Janssen and R. van Roij, Phys. Rev. Lett. **118**, 096001 (2017).

[5]   J. Schiffer, D. Linzen, and D. U. Sauer, J. Power Sources **160**, 765 (2006).

[6]   C. Pean, C. Merlet, B. Rotenberg, P. A. Madden, P. L. Taberna, B. Daffos, M. Salanne, and P. Simon, ACS Nano **8**, 1576 (2014).

[7]   X. Wang, M. Salari, D. Jiang, J. Chapman Varela, B. Anasori, D. J. Wesolowski, S. Dai, M. W. Grinstaff, and Y. Gogotsi, Nat. Rev. Mater. **5**, 787 (2020).

[8]   Y. Dandeville, P. Guillemet, Y. Scudeller, O. Crosnier, L. Athouel, and T. Brousse, Thermochim. Acta **526**, 1 (2011).

[9]   O. Munteshari, J. Lau, A. Krishnan, B. Dunn, and L. Pilon, J. Power Sources **374**, 257 (2018).

[10] M. Janssen, E. Griffioen, P. M. Biesheuvel, R. van Roij, and B. Erné, Phys. Rev. Lett. **119**, 166002 (2017).

[11] A. Likitchatchawankun, R. H. DeBlock, G. Whang, O. Munteshari, M. Frajnkovič, B. S. Dunn, and L. Pilon, J. Power Sources **488**, 229368 (2021).

[12] A. d'Entremont and L. Pilon, J. Power Sources **246**, 887 (2014).

[13] J. E. Vos, D. Inder Maur, H. P. Rodenburg, L. van den Hoven, S. E. Schoemaker, P. E. de Jongh, and B. H. Erné, Phys. Rev. Lett. **129**, 186001 (2022).

[14] A. L. d'Entremont and L. Pilon, J. Power Sources **273**, 196 (2015).

[15] A. C. L. de Lichtervelde, J. P. de Souza, and M. Z. Bazant, Phys. Rev. E **101**, 022406 (2020).

[16] M. Janssen, A. Härtel, and R. van Roij, Phys. Rev. Lett. **113**, 268501 (2014).

[17] A. Härtel, M. Janssen, D. Weingarth, V. Presser, and R. van Roij, Energy Environ. Sci. **8**, 2396 (2015).

[18] P. Pelagejcev, F. Glatzel, and A. Hartel, J. Chem. Phys. **156**, 034901 (2022).

[19] L. Zeng, T. Wu, T. Ye, T. Mo, R. Qiao, and G. Feng, Nat. Comput. Sci. **1**, 725 (2021).

[20] S. K. Reed, O. J. Lanning, and P. A. Madden, J. Chem. Phys. **126**, 084704 (2007).

[21] See Supplemental Material [url] for simulation details, robustness of simulations, details of the modified lattice gas model and electrical double layer structures, and the understanding of translational and orientational entropies, which includes Refs. [2-4], [10], [19-20], [22-26], [34-42].

[22] T. Lazaridis and M. E. Paulaitis, J. Phys. Chem. **96**, 3847 (1992).

[23] I. Borukhov, D. Andelman, and H. Orland, Phys. Rev. Lett. **79**, 435 (1997).

[24] Z. A. H. Goodwin and A. A. Kornyshev, Electrochem. Commun. **82**, 129 (2017).

[25] A. A. Kornyshev, J. Phys. Chem. B **111**, 5545 (2007).

[26] M. V. Fedorov and A. A. Kornyshev, Chem. Rev. **114**, 2978 (2014).

[27] J. Vatamanu, O. Borodin, M. Olguin, G. Yushin, and D. Bedrov, J. Mater. Chem. A **5**, 21049 (2017).

[28] D. Frenkel, Physical A **263**, 26 (1999).

[29] W. Schmickler, Chem. Rev. **96**, 3177 (1996).

[30] M. S. Kilic, M. Z. Bazant, and A. Ajdari, Phys. Rev. E **75**, 021502 (2007).

[31] G. Gonella *et al.*, Nat. Rev. Chem. **5**, 466 (2021).

[32] C.-Y. Wang, T. Liu, X.-G. Yang, S. Ge, N. V. Stanley, E. S. Rountree, Y. Leng, and B. D. McCarthy, Nature **611**, 485 (2022).

[33] Y. Liu, Y. Zhu, and Y. Cui, Nat. Energy **4**, 540 (2019).

[34] B. Hess, C. Kutzner, D. van der Spoel, and E. Lindahl, J. Chem. Theory Comput. **4**, 435 (2008).

[35] U. Essmann, L. Perera, M. L. Berkowitz, T. Darden, H. Lee, and L. G. Pedersen, J. Chem. Phys. **103**, 8577 (1995).

[36] D. J. Evans and B. L. Holian, J. Chem. Phys. **83**, 4069 (1985).

[37] D. E. Smith and L. X. Dang, J. Chem. Phys. **100**, 3757 (1994).

[38] I.-C. Yeh and M. L. Berkowitz, J. Chem. Phys. **111**, 3155 (1999).

[39] G. Feng, J. S. Zhang, and R. Qiao, J. Phys. Chem. C **113**, 4549 (2009).

[40] C. Merlet, M. Salanne, and B. Rotenberg, J. Phys. Chem. C **116**, 7687 (2012).

[41] W. D. Cornell *et al.*, J. Am. Chem. Soc. **117**, 5179 (1995).

[42] L. Scalfi, D. T. Limmer, A. Coretti, S. Bonella, P. A. Madden, M. Salanne, and B. Rotenberg, Phys. Chem. Chem. Phys. **22**, 10480 (2020).